DR.KSHIRSAGAR S.V.

Research Paper in Peer-Reviewed or UGC listed Journals (2020-21)

Sr. No.	Title of Paper with Page No.	Name of Journal	ISSN/ISBN No.	Impact factor, if any	No. of Co-authors	Whether you are the main author
01	Sensors and Health monitoring, pp.11341-11344,	Asian Journal of Science and Technology, Vol. 11, Issue, 11, 2020 Available Online athttp://www.journalajst.com, An International Peer Reviewed Online Journal Published online 30 Nov. 2020	ISSN: 0976-3376,	Impact Factor : 6.946	02	Co-author
02	Magnetic Properties of $MgZn_xTi_xFe_{2-2x}O_4$ System synthesized by Solid-State Reaction Method, pp. 492-497,	IJISET-International Journal of Innovative Science, Engineering & Technology, Vol.8 Issue 3, March **2021,** www.ijiset.com	ISSN(online) 2348-7968,	Impact factor (2020)-6.72	04	Yes(Main author)
03	Stability Constants and Thermodynamic Parameters of Lanthanides (III) Complexes with 5-Bromo, Ortho HydroxyAcetophenone – N – (4'– Methyl Phenyl) Imine	International Journal of Scientific Research in Science and Technology	Print ISSN: 2395-6011 Online ISSN: 2395-602X	6.23	03	Co author
04	SAR Remote sensing for environmental Monitoring.	International Journal of Scientific Research in Science, Engineering and Technology	Print ISSN: 2395-1990 Online ISSN: 2394-4099	6.23	03	Co author

IJISET - International Journal of Innovative Science, Engineering & Technology, Vol. 8 Issue 3, March 2021
ISSN (Online) 2348 – 7968 | Impact Factor (2020) – 6.72
www.ijiset.com

Dr. P. R. Maheshmalkar

Magnetic Properties of $MgZn_xTi_xFe_{2-2x}O_4$ System synthesized by Solid-State Reaction Method

S.V. Kshirsagar[1], C. M. Kale[2]*, P. R. Maheshmalkar[1], S.J. Shukla[3], K. M. Jadhav[4]

[1]Department of Physics, Mrs. K. S. K. College, Beed
[2]Department of Physics, Indraraj Arts, Commerce and Science College, Sillod, Aurangabad
[3]Department of Physics and P. G. Research center, Deogiri College, Aurangabad
[4]Department of Physics Dr. Babasaheb Ambedkar Marathwada University, Aurangabad (M. S.) India -431004

***Corresponding author:** cmkale1973@gmail.com

Abstract

In this work, we have focused on the structural and magnetic properties of $MgZn_xTi_xFe_{2-2x}O_4$ (from x=0.1 to 0.6 in the step of 0.1) spinel ferrite. The samples were synthesized by solid-state reaction method and were characterized by X-ray diffraction (XRD) technique to confirm the formation of single-phase cubic spinel structure. XRD data used to investigate the lattice constant. It is observed that, the lattice constant increases with Zn and Ti concentration 'x'. The magnetic properties were measured with the help of the pulse-field technique. These magnetic properties like saturation magnetization (M_s), magneton number (n_B) both decrease with an increase in Zn, Ti concentration 'x'. The observed and calculated magneton numbers are agreed to close each other for x = 0.0 - 0.3. The discrepancy in magneton number values is observed for the sample x > 0.3 suggesting the canted spin structure of the samples. Curie temperature was determined by Loria techniques and it decreases with the substitution of Zn, Ti concentration 'x'.

Keywords: Spinel ferrite, X-ray diffraction, magnetic properties, Curie temperature.

1. Introduction

Technological advances in a variety of areas have generated a growing demand for the research and application of magnetic materials such as ferrites in devices [1-3]. Ferrites have many applications in high-frequency devices, and they play a useful role in technological and magnetic applications because of their high electrical resistivity and sufficiently low dielectric losses over a wide range of frequencies. The first use of ferrite materials in a power application was to provide the time-dependent magnetic deflection of the electron beam in the television receivers where the two ferrite components used were the deflection yoke and flyback transformer. Magnetic ferrite materials have been drawing much attention because they show unique features such as quantum size effects and magnetic tunneling. They are also important for technological applications, not only in high-density magnetic recording systems but also as a material in the medical field. We studied the

magnetic properties of Ni–Zn ferrite nanoparticles and found remarkable characteristics [4]. The general chemical formula of ferrite possessing the structure of the mineral spinel, $MgAl_2O_4$ is MFe_2O_4. The presence of Fe^{3+}, Fe^{2+}, Ni^{2+}, and Mn^{2+} can be used to provide the unpaired electron spins. Other divalent ions such as Mg^{2+} or Zn^{2+} (or monovalent ions such as Li^{+}) are not paramagnetic but affect the Fe^{3+} ions on the crystal lattice sites to provide or increase the magnetic moment.

The compound $MgFe_2O_4$ is a partly inverted spinel (x =1/3 and y=2/3), which behaves as a collinear ferrimagnet. When the B sites are diluted by Ti, according to the Monte-Carlo simulation of Scoll and Binder [5], it has been observed that the electrical resistivity is markedly changed by controlling the firing temperature, atmosphere, and appropriate type and amount of substituent [6, 7]. The (Fe_xMg_{1-x}) $(Fe_{2y}Mg_{2-2y}Ti_t)$ O_4 system was already studied by magnetic and Mössbauer measurements [8]. An understanding of the mechanism involved in the changes brought about by the addition of substituents provides useful information for the specific application. Abbas et al. [9] studied $Mg_{x+1}Ti_xFe_{2-2x}O_4$ ferrite and found that the compound has a spinel structure. Joshi et al [10] studied the Zn substituted $MgFe_2O_4$ and found interesting results on susceptibility, magnetization, and Mössbauer. The combined effect of Zn and Ti on the properties of Mg ferrite is not reported in the literature. So, this paper, reports the synthesis of Mg–ferrite and, the magnetic behavior of $MgZn_xTi_xFe_{2-2x}O_4$ ferrite was carried out to discuss the role of Ti^{4+} and Zn^{2+} ions substitution.

2. Experimental details

The samples of $MgZn_xTi_xFe_{2-2x}O_4$ spinel ferrite systems with varying x from 0.0 to 0.6 in the step of 0.1 were synthesized by double sintering solid-state reaction method. 99.9 % AR grade oxides of magnesium, zinc, titanate, and ferric were used for the preparation of $MgZn_xTi_xFe_{2-2x}O_4$ ferrite samples. The pre-sintering and final sintering of the samples were carried out at 950^0C and 1100^0C respectively for 12 hours in a muffle furnace. The samples were furnace cooled to room temperature and then the prepared samples were used for further investigations.

All the steps involved in the preparation of ferrites by solid-state reaction method are shown in the following **Fig.1**.

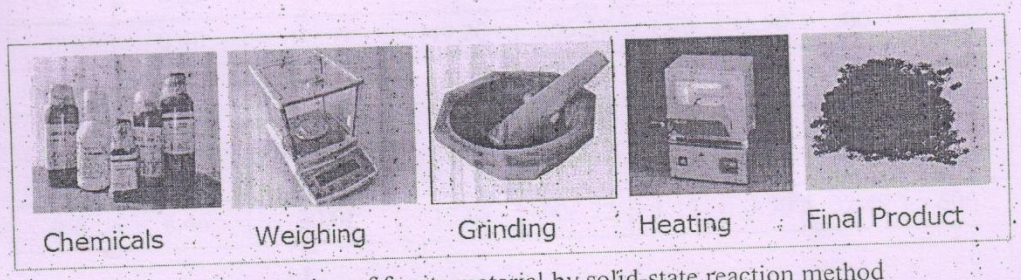

Fig.1. Preparation of ferrite material by solid-state reaction method

The samples were initially characterized by powder X-ray diffraction technique and it has been employed at room temperature. The XRD patterns were recorded in the 2θ range of

20^0-80^0 using Cu-K_α radiation. The magnetic properties were measured using the pulse-field technique provided by Magneta Company.

3. Results and discussion

3.1. X-Ray diffraction

Room-temperature X-ray diffraction (XRD) patterns of all samples of the ferrite system $MgZn_xTi_xFe_{2-2x}O_4$ are depicted in Fig. 2. All the XRD patterns are clean and do not contain any impurity phase. All the peaks in the XRD patterns are assigned by the (hkl) values. The XRD pattern clearly shows the presence of all these reflections belongs to the cubic spinel structure. All these peaks shift towards the right side due to the substitution of Zn and Ti ions. This is confirmed by the change in the interplanar spacing values. The values of interplanar spacing 'd' are used to determine lattice constant 'a' (Table 1) of the spinel ferrite system. The lattice constant increases with the co-substitution of Zn and Ti ions. In the present series of $MgZn_xTi_xFe_{2-2x}O_4$, $2Fe^{3+}$ ions are replaced by combinations of divalent Zn^{2+} ions and tetravalent Ti^{4+} ions. The average ionic radii of Zn^{2+} and Ti^{4+} is quite large than that of Fe^{3+} ions and hence the substitution of Zn, Ti ions in place of Fe^{3+} ions causes the increase in lattice constant of the system $MgZn_xTi_xFe_{2-2x}O_4$. In Zn substituted $MgFe_2O_4$ lattice constant increases with Zn substitution. Similarly in Ti substituted $MgFe_2O_4$ [11] lattice constant increases. With co-substitution of Zn and Ti the lattice constant of the $MgFe_2O_4$ spinel ferrite also increases.

Table.1

Lattice constant and Magnetization Parameters of the system of $MgZn_xTi_xFe_{2-2x}O_4$ ferrite system

Comp. x	Lattice Constant 'a' (Å)	Magnetization Parameter			Magneton Number 'n_B'		Y-K angle 'θ_{YK}'	T_c by Loria Tech.
		Mr (emu/gm)	Ms (emu/gm)	Hc (Oe)	Obs.	Cal.		
0.0	8.37	08.29	32.24	084.06	1.15	1.00	00	665
0.1	8.39	00.47	51.71	023.37	1.85	1.00	00	646
0.2	8.40	05.09	49.20	005.37	1.76	1.50	00	643
0.3	8.42	00.23	18.22	017.52	0.65	2.00	31.81	641
0.4	8.43	00.12	00.85	554.44	1.46	2.50	18.57	632
0.5	8.45	12.76	52.90	033.23	1.09	3.00	30.64	626
0.6	8.46	00.01	13.08	006.72	1.17	3.50	32.49	606

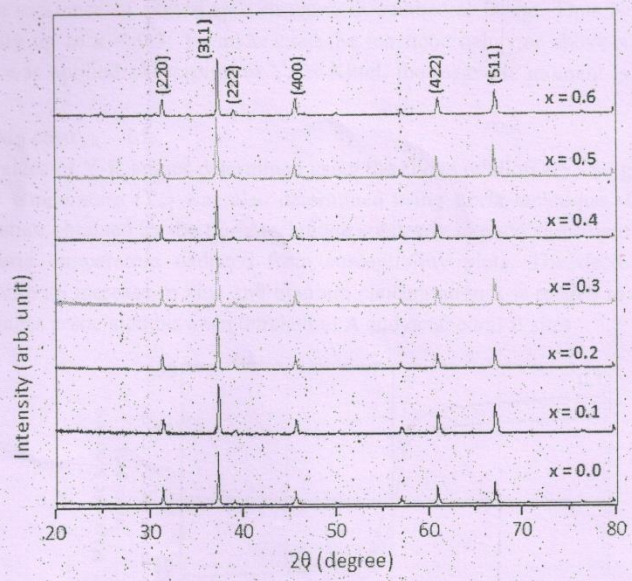

Fig.2. X-ray diffraction patterns of $MgZn_xTi_xFe_{2-2x}O_4$ ferrite system

3.1. Magnetization

The saturation magnetization M_s and magneton number (n_B) the saturation magnetization per formula unit in μ_B was obtained using pulse-field hysteresis loop technique.

Fig. 3 represents the typical M-H plots for the compositions x = 0.1 and x = 0.2 were recorded at room temperature. All these hysteresis loops exhibit ferrimagnetic behavior which reduces by the addition of non-magnetic Zn, Ti ions. These M-H plots are used to obtain the values of coercivity (Hc), remanent magnetizations (Mr), etc, and the values are presented in Table 1.

The values of the magneton number are given in Table 2. It can be seen from the table that magneton number and saturation magnetization both decrease with Zn, Ti concentration x. The compositional variation of magneton number is shown in Fig.4, it shows that magneton number n_B initially increases and then decreases with concentration x. To understand the typical behavior of the magneton number Neel's model has been applied. According to Neel's two sub-lattice models of ferrimagnetism magneton number, n_B is given by the difference in the magnetic moment of tetrahedral A and octahedral B site i.e

$n_B = M_B - M_A$.

The M_B and M_A denote the magnetic moments of B and A sites respectively. The magnetic moments of A and B sites are calculated by taking the ionic magnetic moments of Fe^{3+}, Ti^{4+}, Zn^{2+}, Mg^{2+} as 5 μ_B, 4μ_B, 0μ_B, 0μ_B respectively. Using the cation distribution formula the Neel's magnetic moments were calculated. The observed and calculated magnetic moment agrees close to each other for x=0.0 to x = 0.3. For x > 0.3 it differs from each other

indicating the existence of canted spin structure at octahedral B site. Thus Neel's model is applicable only up to x = 0.3. To understand the magnetic behavior above x = 0.3 Yafet-Kittel model was applied. According to Yafet-Kittel, the magnetic moment is given by the relation

$$n_B = M_B \cos\alpha_{YK} - M_A$$

The values of Y-K angles determined using the above relation are also given in Table 1. The Curie temperature (T_c) was also determined using Loria technique. The values of Curie temperature obtained by the Loria technique are nearly in good agreement [12] with the values of Curie temperature deduced from susceptibility plots. The decrease in Curie temperature with an increase in zinc and titanium concentration x is related to a decrease in magnetic linkages associated between tetrahedral A and octahedral B sites.

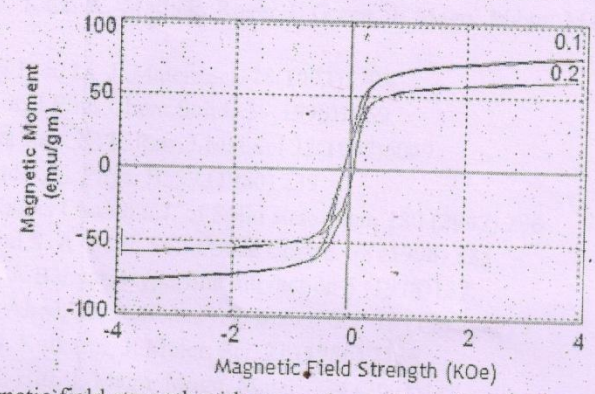

Fig. 3: Variation magnetic field strength with magnetic moments for $MgZn_xTi_xFe_{2-2x}O_4$ system. (Typical sample x = 0.1 and 0.2)

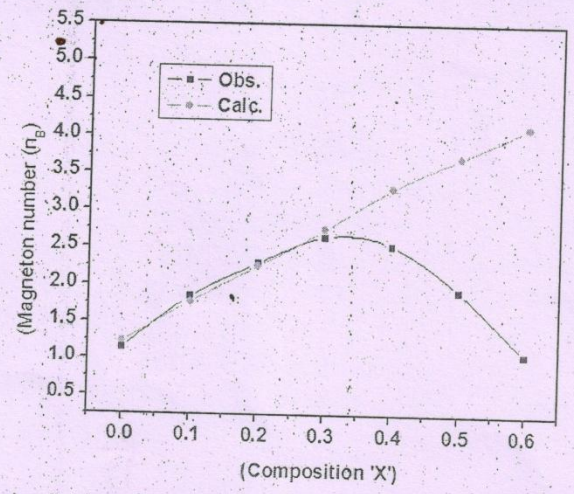

Fig.4: Variation magnetic field strength with magnetic moments for $MgZn_xTi_xFe_{2-2x}O_4$ system

4. Conclusions

The experimental results on the system $MgZn_xTi_xFe_{2-2x}O_4$ led us to conclude.

The analysis of X-ray diffraction patterns revealed the formation of single-phase cubic spinel structure of all the samples under investigation. The lattice constant increases with an increase in Zn, Ti concentration 'x'.The saturation magnetization (M_s), magneton number (n_B) both decreases with increase in Zn, Ti concentration 'x'. The observed and calculated magneton numbers agree close to each other for x = 0.0 – 0.3. The discrepancy in magneton number values is observed for x > 0.3 suggestings canted spin structure of the present samples. Curie temperature determined by various techniques is in good agreement with each other and decreases with the substitution of Zn, Ti concentration 'x'.

References:

1. Philip Shepherd, Kajal K. Mallick, Roger J. Green, J. Magn. Magn. Mater. 311 (**2007**) 83
2. J.H.Liu, L.Wang F. S. Li. J. Mater. Sci. 28(**1993**)1793
3. E.Kester, B.Glliot, J.Phys.Chem.Solids 59(**1998**)1259
4. B. Parvatheewara Rao, K. K.Rao, J.Mat.Sci 32(**1997**)6049
5. F. Scholl, K. Binder, Z. Phys. B, 39 (**1980**) 239
6. Sonal Singhal, Kailas Chandra. J. of Solid state chem 180 (**2007**) 296
7. A. K. Ghatage and S. A. Patil, Solid State Comm. 98 (**1996**) 885
8. N.A.Eissa and A.A.Bahgat, Hyperfine interaction 5 (**1978**)137.
9. Y. Abbas, M. A. Ahed, M. A. Semary, J. Mater. Sci. 18 (1983) 2890
10. H. H. Joshi, R. G. Kulkarni, J. Mater. Sci. 21 (**1986**) 2138
11. M.Aamer, M. El. Hiti. J. Magn. Magn. Mater. 234 (**2001**)118
12. Y. Ichiyanagi, M. Kubota, S. Moritake, Y. Kanazawa, T. Yamada, T. Uehashi. J. Magn. Magn. Mater. 310 (**2007**) 2378

International Virtual Conference on Materials and Nanotechnology
In Association with International Journal of Scientific Research in Science and Technology
Volume 9 | Issue 4 | Print ISSN: 2395-6011 | Online ISSN: 2395-602X (www.ijsrst.com)

Stability Constants and Thermodynamic Parameters of Lanthanides (III) Complexes with 5-Bromo, Ortho Hydroxy Acetophenone – N – (4'– Methyl Phenyl) Imine at 250C

S.B. Maulage[1], S V Gayakwad[1], R G Machale[1], S V Kshirsagar[1]
[1]Mrs. K.S.K. College, Beed, Maharashtra, India

ABSTRACT

Stability constants of some trivalent lanthanides (La, Ce, Pr, Nd, Sm, Gd, Tb, Dy, Yb and Ho) complexes with Schiff base 5-bromo, Ortho hydroxy Acetophenone – N – (4'– methyl phenyl) imine (R_1), have been determined in 50 % (v/v) ethanol-water medium at 25^{0}C and μ = 0.1 M ($NaClO_4$) ionic strength by Irving – Rossotti method. The log K^H and log K values are used to discuss the effect of substituents and atomic size of the trivalent lanthanides. The thermodynamic parameters for the formation of 1:1 and 1:2 complexes have been calculated.

Keywords : Stability Constants, Thermodynamic Parameters, Lanthanides, Schiff Base.

I. INTRODUCTION

Literature survey has revealed that there not enough systematic study has been recorded so far on the trivalent lanthanide complexes of Schiff base derived from 5-bromo, ortho hydroxy acetophenone – N – (4'– methyl phenyl) imine. The objective of the present investigation is to ascertain the coordination behavior of this Schiff base towards lanthanides (III) ions in 50 % (v/v) alcohol-water medium. The observed values of stability constants of these complexes have been explained on the basis of ionic size of the metals, basicity of ligand, gadolinium break and tetrad effect. The changes in thermodynamic parameters are used to explain the stability of these complexes.

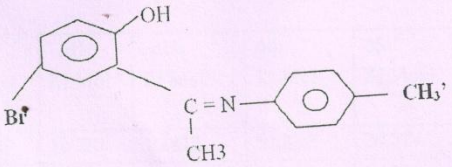

II. EXPERIMENTAL

All the chemicals used for the synthesis of bidentate ligand and their complexes were AR grade. The Schiff base 5-bromo, ortho hydroxy acetophenone – N – (4'– methyl phenyl) imine was synthesized by reported method.[3] The solutions of lanthanide complexes were prepared in the double distilled water and standardized.[4] The initial ionic strength of all the solutions was maintained at 0.1 M by $NaClO_4$. An Elico LI – 120 P^H meter in conjunction with a combined electrode was used. The measurements

(237)

were made at 25° C (±0.01°) and μ = 0.01M $NaClO_4$ in 50 % aqueous ethanol. The log K^H and log K values were computed by half – integral method, point wise calculations and also by the method of least squares. The average log K values were used to calculate ΔG from the Van't Hoff's isotherm. The ΔH and ΔS values were calculated from the Van't Hoff's isochore and the equation ΔG = ΔH - TΔS, respectively. The data are listed in Table – 2.

The pK_1 and pK_2 values of synthesized Schiff base 5-bromo, ortho hydroxy acetophenone – N – (4'– methyl phenyl) imine which represent the de-protonation of NH group at azomethine nitrogen atom and phenolic OH group were determined at n_A = 1.5 and 0.5 respectively. The values were further checked from the plots of log $[(2-n_A)\sqrt{(n_A-1)}]$ vs B and log $n_A/(1-n_A)$ vs B (B = pH meter reading) and are given in Table -1. The pK_1 value of ligand is lower since it is having bromo substituent at *para* position to amino group. This can be attributed on the basis of domination nature of -M effect of bromide group.

Table – 1: Complex formation of lanthanides (III) with 5-bromo, ortho hydroxy acetophenone – N – (4'– methyl phenyl) imine

Temp →		25 °C
Ligand	pK_1	4.66
	pK_2	9.74

III. RESULTS AND DISCUSSIONS

Table – 2: Stability constants and thermodynamic parameters of lanthanides (III) complexes of bidentate Schiff base 5-bromo, ortho hydroxy acetophenone – N – (4'– methyl phenyl) imine at 25° C ± 0.02° C and 0.1 M $NaClO_4$.

Complexes	log K_1	log K_2	$-\Delta G_1$ KJ Mol^{-1}	$-\Delta G_2$ KJ Mol^{-1}	$-\Delta H_1$ KJ Mol^{-1}	$-\Delta H_2$ KJ Mol^{-1}	ΔS_1 KJ Mol^{-1}	ΔS_2 KJ Mol^{-1}
La (III)	5.99	4.46	34.179	25.449	18.731	16.412	51.839	30.324
Ce (III)	6.13	4.66	34.978	26.590	13.791	17.552	71.099	30.329
Pr (III)	6.33	5.14	36.119	29.329	15.231	12.765	70.095	55.584
Nd (III)	6.39	5.23	36.462	29.843	15.414	17.036	70.631	42.976
Sm (III)	6.45	5.32	36.804	30.356	16.455	13.677	68.286	55.971
Eu (III)	6.58	5.59	37.546	31.897	11.584	17.682	87.120	47.700
Gd (III)	6.17	5.26	35.206	30.014	14.913	19.973	68.099	33.694
Tb (III)	6.28	5.38	35.834	30.699	12.067	15.018	79.756	52.621
Dy (III)	6.62	5.87	37.774	33.495	15.956	12.644	73.214	69.967
Ho (III)	6.25	5.36	35.663	30.584	13.962	18.530	72.823	40.451

*Standard deviation for log K_1 and log K_2 are ± 0.019 and ± 0.035 respectively.

The shielding of the *4f* –electrons is exhibited in the stability constants of the present rare earth complexes, which shows very little difference in these values with the increase in atomic number. In these complexes the rare earth metal ions bind predominantly to oxygen and weakly to nitrogen of the Schiff bases.[2] These complexes show a regular increase of stability constants from La (III) to Eu (III) with a discontinuity of Gd (III) and Tb (III) which is commonly known as gadolinium break. After Tb (III), stability constant increases up to Dy (III) and then decreases for Ho (III) as shown in Table – 2. This shows occasional maxima and minima after gadolinium break. In all cases, Gd (III) and Eu (III)

chelates have lower value of log K_1 in relation to those of Dy (III) to Ho (III) chelates.

The change in free energy is directly related to log K values. The stability constants of trivalent La, Ce, Pr, Nd, Sm, Eu, Gd, Tb, Dy, and Ho complexes with 5-bromo, ortho hydroxy acetophenone – N – (4'–methyl phenyl) imine follows the order Dy > Eu > Sm > Nd > Pr > Tb > Ho > Gd > Ce ≥ La. These stabilities are similar to the observations made by number of workers. [7-10] and are accordance with Irving – Williams orer.[11] The thermodynamic parameters for lanthanide complexes with Schiff base were obtained from log K_1 and log K_2 at 25°C temperature. It seems that the log K_1 and log K_2 values decrease with increase in temperature, indicating that the high temperature does not favour the formation of stable complexes. The ΔH_1 and ΔH_2 values are all negative, while ΔS_1 and ΔS_2 are all positive. The resulting ΔG_1 and ΔG_2 values are all negative. The more negative values of ΔG_1 and ΔG_2 indicate that the 1:1 and 1:2 complex formation is thermodynamically favored. The negative values of ΔH_1 and ΔH_2 also lead to the same inference. The entropy effect is found to be predominant over the enthalpy effect which is indicated by the high positive values of entropy.

IV. REFERENCES

[1]. S. M. Irving and H.S. Rossotti, J. Chem. Soc.,2904 (1954).

[2]. V. Mishra and M. C. Jain. Indian Chem. Soc., 1988. 65. 380.

[3]. T.K. Chondhekar and D.D. Khanolkar, Indian J. Chem., Sect. A. 1986,25, 868.

[4]. H. Flaschka, Microchim. Acta, 1955, 55.

[5]. A Syamal, Coord, Chem, Rev., 16, 309 (1985).

[6]. M.S. Mayadeo, S.S. Purohit and S.H. Hussain, J. Indian Chem. Soc., 1982, 59, 894.

[7]. H.L. Kalara, K.E. Jabalpurwala and K.A. Venkatchalam., Inorg. Nucl. Chem. Lett., 26, 1027 (1964).

[8]. R. G.Pearson and F. Basolo, Mechanism of Inorganic reactions:study of complexesin solution, John Wiley, New York, Vol 9, p.16 (1958).

[9]. K.T.Kendre, N.R.Manjaramkar and Y.H. Deshpande, J.Indian Chem. Soc.,63, 615 (1986).

[10]. D.V.Jahagirdar and D. D. Khanolkar, Indian J. Chem., 13,168 (1975).

[11]. H. Irving and R.J.P. Williams, Nature (London), 162,746 (1948).

International Journal of Scientific Research in Science, Engineering and Technology
Print ISSN: 2395-1990 | Online ISSN : 2394-4099 (www.ijsrset.com)

SAR Remote Sensing for Environmental Monitoring

Pradnya R Maheshmalkar[1*], Shafiyoddin B Sayyad[2], Shivanand V Kshirsagar[1], Kirti R Desai[3]
[1]Department of Physics, Mrs. K. S. K. College, Beed, Maharashtra, India
[2]Department of Physics, Milliya College, Beed, Maharashtra, India
[3]Department of Physics, Balbhim College, Beed, Maharashtra, India

Article Info
Volume 9, Issue 5
Page Number: 46-51

Publication Issue :
July-August-2021

Article History
Accepted : 02 July 2021
Published: 25 July, 2021

ABSTRACT

This paper describes the satellite resources and advances in remote sensing for environmental planning, monitoring and management. Satellites provide a great deal of the remote sensing imagery commonly used today. Remote-sensing technologies have been applied widely in environmental monitoring, in agriculture for Improvement of a Crop /soil status, climate change detection, flood prediction, mapping etc.,. Remote sensing is a popular technique that is using in the mapping and monitoring of earth features. Sensors will progressively provide a better understanding of our activities in urban as well as rural areas. The advancement allow for monitoring earth features can be derived from the spectral properties of remotely-sensed imagery. Synthetic Aperture Radar can be used to retrieve information about some physical parameters of the targets under study by using electromagnetic radiations. This review provides the basis for the discussion, of the applicability of the SAR Remote Sensing for environmental monitoring.

Keywords: Remote Sensing, SAR, Environment

I. INTRODUCTION

Remote sensing is the art and science of deriving useful information from imagery and other data acquired from a distance. The implementation of Remote Sensing requires better understanding of sustainable environmental management. A wide variety of remote sensing systems are used today to provide information about the earth, its atmosphere, oceans, and land surfaces. Remote sensing can efficiently monitor the environment and provide a scientific basis for the valuable re-establishment of the environment. Many environmental indicator based on remote sensing are estimated to reflect environmental status.

SAR is a type of active data collection where a sensor produces its own energy and then records the amount of that energy reflected back after interacting with the Earth. Problems associated with environmental factors in almost all parts of the globe. Knowledge about the management of these problems is important

for any task planning in order to satisfy the environmental conditions.

The natural environment is essential for human survival and development since it provides water resources, land resources, biological resources and climate resources etc. The development trend and future directions are put forward to direct the research and application of environmental monitoring and protection in the new era. Global and regional environmental monitoring relies heavily on remote sensing satellite and sensors which are capable of quickly collecting spatial and spectral information of large-extent entities on the Earth's surface. With the fast development of space technologies, remote sensing data are becoming more and more abundant [1]. SAR is an active radar technology that senses microwave signals reflected off Earth's surface, which means SAR imagery can be created day or night and in virtually any kind of weather. The result is cloud-free, high-contrast imagery. After the radar sends its microwave signal toward a target, the target reflects part of the signal back to the radar antenna. This reflection is called "backscatter." Various properties of the target (land, water, trees, etc.) affect how much the target backscatters the return signal [2]. SAR has a significant advantage over optical sensors because it can acquire data in poor weather conditions; therefore, it has special value in the field of agricultural remote sensing [3] .

In this paper the identification and characterization of environmental features from polarimetric SAR images has been addressed. This review also updates the discussion on opportunities for future research, applying existing methods to recent advances in technology and planned globe observation task.

II. THEORETICAL BACKGROUND

Most remote sensing devices detect variations in electromagnetic energy. The electromagnetic spectrum is the range of all types of electromagnetic energy according to frequency or wavelength, ranging from shorter wavelengths (ultraviolet) to longer wavelength (near infrared, thermal, microwave). A spectral signature is the degree to which energy is reflected in different regions of the spectrum by different Earth surface materials, enabling them to be detected by visual or digital means from remotely sensed imagery. Finding distinctive spectral response patterns is the key to most procedures for computer-assisted interpretation and digital processing of satellite images [4]. Satellite imagery is made possible by remote sensing instruments that measure energy across the electromagnetic spectrum.

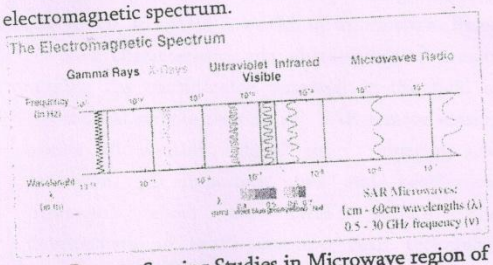

Fig. 1. Remote Sensing Studies in Microwave region of the EM Spectrum

Electromagnetic radiation in the microwave wavelength region is used in remote sensing to provide useful information about the Earth's surface (atmosphere, land and ocean). A microwave imaging system which can produce high resolution image of the earth is the synthetic aperture radar (SAR). The intensity in a SAR image depends on the amount of microwave backscattered by the target and received by the SAR antenna [5]. With the rapid development of different remote sensing satellites capturing information from the earth by sensing energy in different portions of the electromagnetic spectrum, complementary information about the area captured by different satellites is available [6]. SAR uses the microwave range for remote sensing. It works on the longer wavelength range as compared to optical images. Hence, it can penetrate through cloud and vegetation cover. SAR gives the surface characteristics and moisture content. SAR was developed to improve

the azimuth resolution of the RADAR systems. SAR can provide a quantitative estimation of ground changes and can be used in all weathers. PInSAR (Polarimetric SAR) is used in land cover classification and change detection. Limitation of SAR is that it gives less accuracy in dense vegetation and also affected by seasonal changes [7].

III. LITERATURE REVIEW

Several research studies showed the fundamentals of electromagnetic radiation, its interactions with the Earth's surface and atmosphere, as well as development and applications of remote sensing. Many scholars carried out studies based on the SAR Remote Sensing.

Physics is the most fundamental of all the sciences and scientific developments or technologies. Applied physics does the role of their application to modern technologies. Applied physics describes the laws and phenomenon of nature with their application in different fields like Physics of imaging, Atmospheric Physics, Nanotechnology, Remote Sensing etc. Electromagnetic radiation in the microwave wavelength region is used in remote sensing to provide useful information about the Earth's surface (atmosphere, land and ocean). A microwave imaging system which can produce high resolution image of the earth is the synthetic aperture radar (SAR). The intensity in a SAR image depends on the amount of microwave backscattered by the target and received by the SAR antenna [5]. Probably the most important area in which data from remote sensing can be used is that of regional and global monitoring of changes in land use, vegetation cover and environmental media. Earth observation systems are most suited for delivering information for such monitoring purposes as they cover extensive areas. They record regularly and guarantee comparable information over long periods of time (e.g. from Landsat). Remote sensing data are an important basis for dealing with questions in landscape ecology. It makes it possible to get current information on large areas of land. Used alongside visual evaluation and superimposing other geographical data it is possible to classify land use areas as well as carry out a whole range of other thematic evaluations. The information from remote sensing data for landscape ecology comes from different regions of the spectrum, depending on the backscattering properties of different surface materials such as soil, vegetation type or areas of water and the sensor used [8]. SAR remote sensing can use different imaging parameters, such as the incident angles and the polarization configurations of the sensor, to obtain a wealth of information. Based on these characteristics and advantages, SAR remote sensing has considerable potential in the field of agricultural remote sensing [9]. SAR remote sensing allows all weather, global scale imaging and estimation of important bio and geophysical parameters about the Earth's surface. The development of multi-parameter SAR techniques such as Polarimetric SAR (POLSAR) and Polarimetric Interferometric SAR (POLinSAR) is advancing rapidly, and these novel radar technologies are constantly extending decisively the range of applications of radar in remote sensing. Due to the polarimetric radar sensors (ENVISAT ASAR, ALOS-PALSAR, TerraSAR-X and RADARSAT-2), it is now shown that the accelerated advancement of POLSAR techniques is of direct relevance and of priority to local-to-global environmental ground-truth measurement and validation, stress assessment, and stress-change monitoring of the terrestrial and planetary covers. POLSAR and POLINSAR remote sensing techniques offer efficient and reliable means of collecting information required to extract biophysical and geophysical parameters about the Earth's surface and have found successful applications in crop monitoring and damage assessment, in forestry clear cut mapping, deforestation and burn mapping, in land surface structure (geology) land cover (biomass) and land use, in hydrology (soil moisture, flood delineation), in sea ice monitoring, in

oceans and coastal monitoring (oil spill detection) etc.,[10]. A Polarimetric SAR system measures the backscattered energy of the targets in the scene, including its polarization state. The interaction of the transmitted wave with a scattering object transforms its polarization. Polarization signature is a graphical representation of the backscattered power received from a target, as a function of the polarizations of the incident and scattered electromagnetic waves. A tool named "POLSIC", with basic capability to calculate and represent 3D Polarimetric signatures (Co-polarized and Cross polarized) has been developed, still in an experimentation phase, in order to encourage and develop Polarimetric signature studies of various possible targets/class [11]. Remote sensing techniques based on identifying temporal changes have been trialed on data acquired from the LANDSAT Thematic Mapper (TM), a sensor with moderate spatial resolution (i.e.,12–50 meter pixel size) and medium temporal resolution (i.e., 4–16 day revisit time). The technique trialed on LANDSAT TM data aimed to map the visible indirect temporal land changes associated with illegal waste disposal . These visible indirect temporal land changes include thermal anomalies and/or vegetation stress. Land degraded by the presence of illegal waste is usually noticeable for its spectral signature stability over time in comparison to other features such as urban areas, sea, salt evaporation pools, cultivation systems, etc. [12]

Polarimetric SAR (PolSAR) is a well established technique, which allows the identification and separation of scattering mechanisms in the polarization signature for purposes of classification and parameter estimation. Polarimetric SAR (PolSAR) is sensitive to the orientation and characters of object and polarimetry could yield several new descriptive radar target detection parameters and lead to the improvement of radar detection algorithms. Target decomposition theory has been used for information extraction in PolSAR and it can also explore the phase message in PolSAR data [13]. An attempt has been to develop a Polarimetric Signature Calculation and Visual Representation Tool assigned name "POLSIC", to generate Co-polarized and Cross polarized signatures, based on the calculation of Stokes Matrix and the backscattered power at various ellipticity and orientation angles. The input parameters required for the developed tool, are the amplitude and phase values of all the four polarizations, for each target using any quadpol radar imagery. In this study, RADARSAT-2 imagery has been used to obtain the amplitude and phase values of each target, in all four polarization states. Polarimetric signatures were generated for various urban targets using the developed tool. Vegetated land, built up in the city, built up within lake, and road were found to have an overall higher polarimetric response (backscattered power) as compared to grass lawn, fallow land and minimum in case of water body. Such Polarimetric responses were obtained due to factors like surface roughness and orientation of the target with respect to the radar look angle. The shape of the signature also indicates the scattering characteristics [11]. Different remote sensing datasets, e.g., Landsat TM&OLI, Gaofen-1 and MODIS, have different characteristics, such as spatial resolution, spectral range and resolution. Remote sensor monitoring of soil pollution is mainly based on hyper spectral images, because the hyper spectral remote sensing is able to obtain the quantitative information of soil composition (e.g., organic matter, minerals) due to the characteristics of high spectral resolution. Vegetation indexes are effective and empirical indicators that reflect the status of vegetation on the ground and describe ecological conditions. Soil moisture is a key component of the global water and energy exchange among hydrosphere, atmosphere and biosphere. Vegetation moisture is an indicator reflecting the growth of vegetation [14].

The change in land use from rural to urban is monitored to estimate populations, predict and plan direction of urban sprawl for developers, and monitor adjacent environmentally sensitive areas or hazards.

Temporary refugee settlements and tent cities can be monitored and population amounts and densities estimated. Analyzing agricultural vs. urban land use is important for ensuring that development does not encroach on valuable agricultural land, and to likewise ensure that agriculture is occurring on the most appropriate land and will not degrade due to improper adjacent development or infrastructure. Remote sensing methods can be employed to classify types of land use in a practical, economical and repetitive fashion, over large areas [15].

Currently available satellite imagery has been applied to numerous applications in disaster prediction, investigation and/or management at global, regional and local scales. The data have been mostly used for more detailed assessments of an event's aftermath and reconstruction, as well as in post-disaster scientific research [16].

IV. DISCUSSION AND CONCLUSION

Various opportunities provided by recent advances in technology and data acquisition. Recent advances in Remote Sensing techniques and availability of satellite data **are needed for global, regional and local environmental monitoring.** Remote sensing data can be used for various applications i.e., for monitoring of earth resources, Retrieval of earth surface parameters, Management of earth surfaces etc .The usefulness of remote sensing technique will be improved if the capabilities are operated through the Microwave Synthetic Aperture Radar Imaging. SAR remote sensing is an imaging active microwave remote sensing technique which provides higher spatial resolution data. Interpretation and analysis of remote sensing imagery involves the identification and /or measurement of various targets in an image in order to extract useful information about them. In general, it is clear from this review paper that SAR remote sensing is now prominent potential towards accurate technique for environmental conservation management. In future, remote sensing tools will be highly useful not only for decision making but also understanding the global change issue of earth surfaces. Satellite imagery is a great data source for quickly responding to different emergency events.

This paper concludes that SAR remote sensing has great potential and will play a more significant role in the Environmental Monitoring.

V. REFERENCES

[1]. Jun Li, Yanqiu Pei, Shaohua Zhao, Rulin Xiao, Xiao Sang, Chengye Zhang, A Review of Remote Sensing for Environmental Monitoring in China, Remote Sens. (2020), 12(7), 1130.

[2]. https://www.asf.alaska.edu/asf-tutorials/sar-basics/.

[3]. Liu Chang -an, Chen Zhong-xin, Shao yun, Chen Jin -somg, Tuya Hasi, Pan Hai-zhu, Research advances of SAR remote sensing for agriculture applications: A review, Journal of Integrative Agriculture, (2019), 18 (3):506-525.

[4]. https://www.spacelegalissues.com/

[5]. Arbind Kumar Shah, "Remote Sensing"-A part of an Applied Physics, The Himalayan Physics, Vol.4, No.4, (2013), 102-108

[6]. Samadhan C. Kulkarni, Priti P. Rege, Pixel level fusion techniques for SAR and optical images: A review, Information Fusion 59 (2020), 13-29, journal homepage: www.elsevier.com/locate/inffus.

[7]. S. Agrawal , G. B. Khairnar, A Comparative Assessment Of Remote Sensing Imaging Techniques: Optical, Sar And Lidar, The International Archives of the Photogrammetry, Remote Sensing and Spatial Information Sciences, Volume XLII-5/W3, (2019),1-6 Capacity Building and Education Outreach in Advance Geospatial Technologies and Land Management, 10–11

[8]. https://www.researchgate.net/publication/256307366]

[9]. Liu Chang -an, Chen Zhong-xin, Shao yun, Chen Jin -somg, Tuya Hasi, Pan Hai-zhu, Research advances of SAR remote sensing for agriculture applications: A review, Journal of Integrative Agriculture, (2019), 18 (3):506-525

[10]. https://www.researchgate.net/publication/224116520

[11]. Prof. Anjana Vyas, Ms.Bindi Sashtri, SAR Polarimetric Signatures for Urban Targets - Polarimetric Signature Calculation and Visualization, International Archives of the Photogrammetry, Remote Sensing and Spatial Information Sciences, Vol.XXXIX-B7,,XXIIISPRS Congress,(2012)535-540

[12]. Katharine Glanville and Hsing-Chung Chang, Remote Sensing Analysis Techniques and Sensor Requirements to Support the Mapping of Illegal Domestic Waste Disposal Sites in Queensland, Australia, Remote Sens. (2015), 7, pp.13053-13069]

[13]. Lamei Zhang, Junping Zhang, Bin Zou and Ye Zhang, Comparison of Methods for Target Detection and Applications Using Polarimetric SAR Image, PIERS Online, (2008), Vol. 4, No.1, https://www.researchgate.net/publication/266269817.

[14]. Jun Li, Yanqiu Pei, Shaohua Zhao, Rulin Xiao, Xiao Sang, Chengye Zhang, A Review of Remote Sensing for Environmental Monitoring in China, Remote Sens. (2020), 12(7), 1130; https://doi.org/10.3390/rs12071130

[15]. Fundamentals of Remote Sensing, A Canada Centre for Remote Sensing Remote Sensing Tutorial

[16]. https://www.researchgate.net/publication/230674340